

Free Volume Holes of Rubbery Polymers Probed by Positron Annihilation

Ken-ichi OKAMOTO,* Kazuhiro TANAKA, Mikio KATSUBE, Hidetoshi KITA, and Yasuo ITO†
Department of Advanced Materials Science and Engineering, Faculty of Engineering, Yamaguchi University,
Ube, Yamaguchi 755

† Research Center for Nuclear Science and Technology, The University of Tokyo, Tokaimura, Ibaragi 319-11
(Received August 19, 1992)

The lifetime and the intensity of ortho-positronium (*o*-Ps), τ_3 and I_3 , respectively, were measured for various polymers below and above glass transition temperatures T_g . The average size of micro-vacancies probed by *o*-Ps, $v_{h,Ps}$, was evaluated from τ_3 using an empirical equation. Both temperature dependence of τ_3 and comparison of magnitude of $v_{h,Ps}$ between the polymers and molecular liquids having similar cohesive energy density reveal that the micro-vacancies probed by *o*-Ps at temperatures not much above T_g are pre-existing and momentarily frozen free volume holes rather than Ps bubbles. A method to evaluate the volume fraction and the concentration of free volume holes probed by *o*-Ps, $V_{F,Ps}$, and $C_{h,Ps}$ respectively, is proposed by assuming that the size-distribution is approximated by an exponential function with a mean size $\langle v_h \rangle$, and that the volume fraction of total free volume holes is equal to fractional free volume calculated by the Bondi method. This model predicts clear correlations between $\langle v_h \rangle$ and the concentration of total free volume holes and also between $V_{F,Ps}$ and $v_{h,Ps}$. There is no clear correlation between $C_{h,Ps}$ and I_3 , suggesting that I_3 is not a good measure of the concentration of free volume holes.

Positron annihilation (PA) in polymers has recently attracted much interest because PA is expected to bring forth information about their microstructure.¹⁾ PA lifetime spectra of polymers have a long-lived component which is ascribed to ortho-positronium (*o*-Ps) formed and annihilated in amorphous region. The lifetime of *o*-Ps, τ_3 , is considered to be a good measure of the size of the micro-vacancies where *o*-Ps is trapped.^{1–3)} Spherical holes larger than 0.033 nm³ (ca. 0.4 nm in diameter) can accommodate *o*-Ps. However, it is not clear whether the micro-vacancies seen by *o*-Ps in rubbery polymers are the pre-existing free volume holes large enough to accommodate *o*-Ps or the bubbles formed around Ps as in liquids. Kobayashi et al. have recently suggested that Ps bubbles are formed not only in rubbery polymers but also in glassy ones.⁴⁾ The intensity of the long-lived component, I_3 , is sometimes considered to be a measure of the number of such micro-vacancies.^{1,5,6)} However, it is not mature to correlate I_3 with the number of such vacancies.

In this study, PA properties of various polymers were examined over a wide temperature range above and below the glass transition temperatures, T_g , to clarify the nature of micro-vacancies probed by *o*-Ps.

Experimental

The samples used in this study are as follows; polydimethylsiloxane (PDMS), polyethylene (PE), polypropylene (PP), 1,2-polybutadiene (1,2-PB), Poly(4-methylpentene-1-co- α -olefine) (P4MP-C), poly(ethylene terephthalate) (PET), poly(vinyl acetate) (PVAC), poly(styrene) (PS), poly(methyl acrylate) (PMA), and poly(buthyl methacrylate) (PBMA). The additive-free films of PDMS, PE, PP, P4MP-C, and PET were supplied from Shin-etsu Chemical Industries Ltd., Ube Industries Ltd. (PE and PP), Mitsui Petrochemical Industries Ltd., and Mitsubishi Plastics Ltd., respectively. P4MP-C is a copolymer of 4-methylpentene-1 with a small content of α -olefine (C₁₈ component).

Amorphous PET films (Diafoil) were heat-treated at 408 K for 10 h in vacuo. 1,2-PB supplied from Japan Synthetic Rubber Ltd. was purified by repeated reprecipitations (toluene/methanol). PVAC, PS, PMA, and PBMA were prepared by solution polymerization using azobisisobutyronitrile as an initiator, and isolated by fractional precipitation. Their high-molecular-weight fractions were purified by repeated reprecipitations. Films of these polymers were cast from their benzene solutions onto glass plates. They were dried at 323 K (300 K for PMA) for 20 h in vacuo.

Differential scanning calorimetry (DSC) was measured with a thermal analyzer (Seikodenshi DSC220C) at a heating rate of 10 K min⁻¹. The density ρ was measured by the floating method using potassium iodide-water (for $\rho > 1$ g cm⁻³) or potassium iodide-methanol (for $\rho < 1$ g cm⁻³) solutions. The thermal expansion coefficient was measured with a thermal analyzer (Rigaku Thermal analyzer TAS 100) at a heating rate of 5 K min⁻¹ with a load of 1 g.

The PA lifetime measurements were carried out at the Inter-University Laboratory for the Common Use of JAERI facilities.⁷⁾ The sample films (1×1 cm² wide and 30 to 200 μ m thick) were stacked to make 1 mm thickness. The positron source, 25 μ Ci of ²²NaCl sandwiched between thin nickel foils (2.8 mg cm⁻² thick and 0.5×0.5 cm² wide), was sandwiched by two equivalent stacks of sample films. The sample thus prepared was put in the sample holder of a cryostat. The cryostat was evacuated and the PA lifetime was measured at temperatures below and above T_g . The PA lifetime spectrometer was the fast-fast coincidence equipment with the time resolution of 0.30 ns (FWHM).⁷⁾ Each PA lifetime spectrum, having more than one million total count, was analyzed into three lifetime components using the computer program PATFIT.⁸⁾

Results and Discussion

Characterization. Characterization results for the polymers are listed in Table 1. Judging from the X-ray diffraction patterns, PVAC, PS, PMA, and PBMA are amorphous. Other polymers are semicrystalline.

Table 1. Characterization Results of Polymer Films

No.	Polymers	T_g K	T_m K	ρ g cm ⁻³	ϕ_a —	$\alpha_g^{c)}$ 10 ⁻⁴ K ⁻¹	$\alpha_l^{c)}$ —	CED J cm ⁻³	$V_F^{d)}$ —	$V_F^{e)}$ —
1	PDMS	152	224	0.974	1.0	3.84	8.61	230	—	—
2	1,2-PB	249	364	0.900	0.85 ^{a)}	1.93	6.5	378	0.200	0.175
3	PE	251	384	0.910	0.63 ^{a)}	2.8	7.5	307	0.192	0.180
4	PP	269	437	0.888	0.57 ^{a)}	1.59	5.79	269	0.195	0.181
5	PMA	280	—	1.209	1.0	2.7	5.6	467	0.159	0.151
6	P4MP-C	295	496	0.835	0.65 ^{b)}	3.71	7.38	267	0.209	0.207
7	PBMA	307	—	1.051	1.0	4.02	6.45	374	0.164	0.167
8	PVAC	304	—	1.190	1.0	1.71	5.06	467	0.176	0.177
9	PET	361	527	1.376	0.67 ^{a)}	2.47	6.20	645	0.149	0.162
10	PS	377	—	1.045	1.0	2.11	5.57	466	0.180	0.194

a) Determined from the density, using the values of ρ_a and ρ_c in Ref. 9. b) Determined from the X-ray diffraction pattern. c) The values for P4MP-C and PET were determined in this study. The values for PDMS, 1,2-PB, and the others were cited from Refs. 10, 11, and 9, respectively. d) at 298 K. e) at T_g .

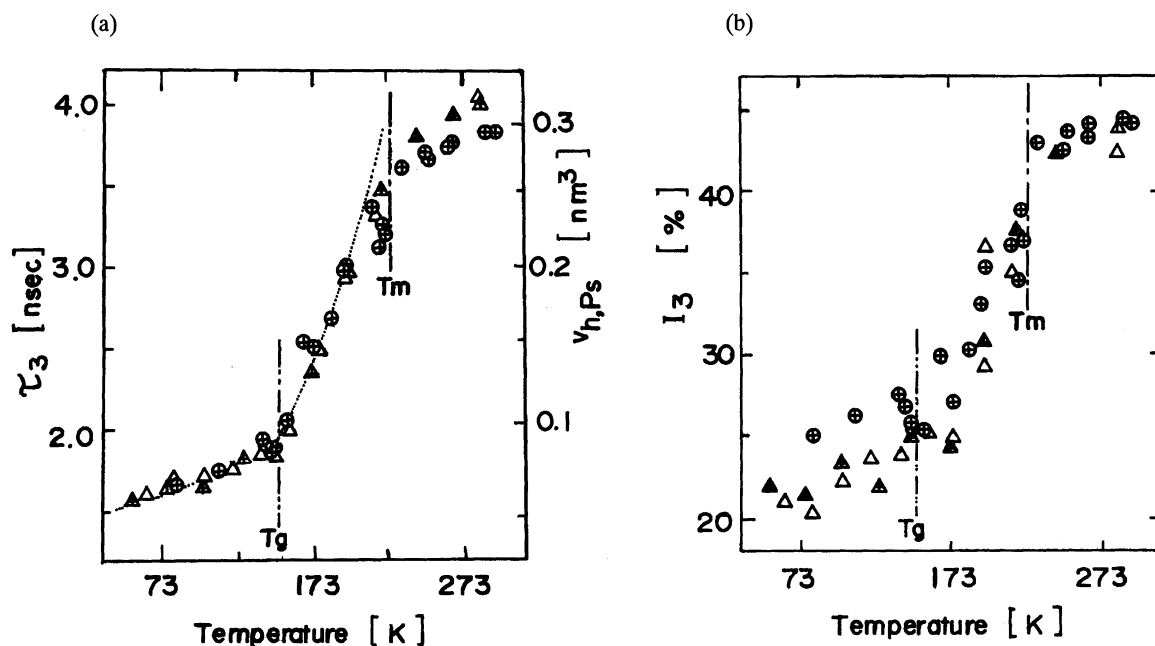


Fig. 1. Temperature dependence of τ_3 and I_3 for PDMS. Triangle and circle symbols were obtained for the different samples cut from the same film using two different equipment sets. \oplus and Δ : 1st cooling run; \triangle : 1st heating run.

The amorphous fraction ϕ_a was calculated from Eq. 1 using the literature values⁹⁻¹¹⁾ for the density of crystalline and amorphous phases, ρ_c and ρ_a , respectively.

$$\phi_a = 1 - (\rho - \rho_a) / (\rho_c - \rho_a) \quad (1)$$

The cohesive energy density (CED) was calculated by the group contribution method of van Krevelen.¹²⁾ The fraction of "free space" V_F refers to the ratio of the so-called "expansion volume"¹³⁾ to the observed volume and was calculated by

$$V_F = (V_T - V_0) / V_T \quad (2)$$

where V_T is the molar volume at temperature T and V_0 is the volume occupied by the molecules at 0 K per

mole of repeat unit of the polymer. V_T was calculated using the values of the molar volume observed at 298 K and the thermal expansion coefficients below and above T_g , α_g , and α_l , respectively. V_0 was estimated to be 1.3 times¹³⁾ the van der Waals volume calculated by the group contribution method of Bondi.¹⁴⁾

Temperature Dependence of τ_3 and I_3 . Figure 1 shows the temperature dependence of τ_3 and I_3 for PDMS. Both τ_3 and I_3 increased with temperature, and displayed dramatic changes at T_g . At the melting point ($T_m=224$ K), τ_3 increased continuously, while I_3 showed a small stepwise increase. A higher-temperature transition was observed at ca. 240 K, where both τ_3 and I_3 started to levell off. Similar higher-temperature transition has been reported for glass-forming liquids¹⁵⁾

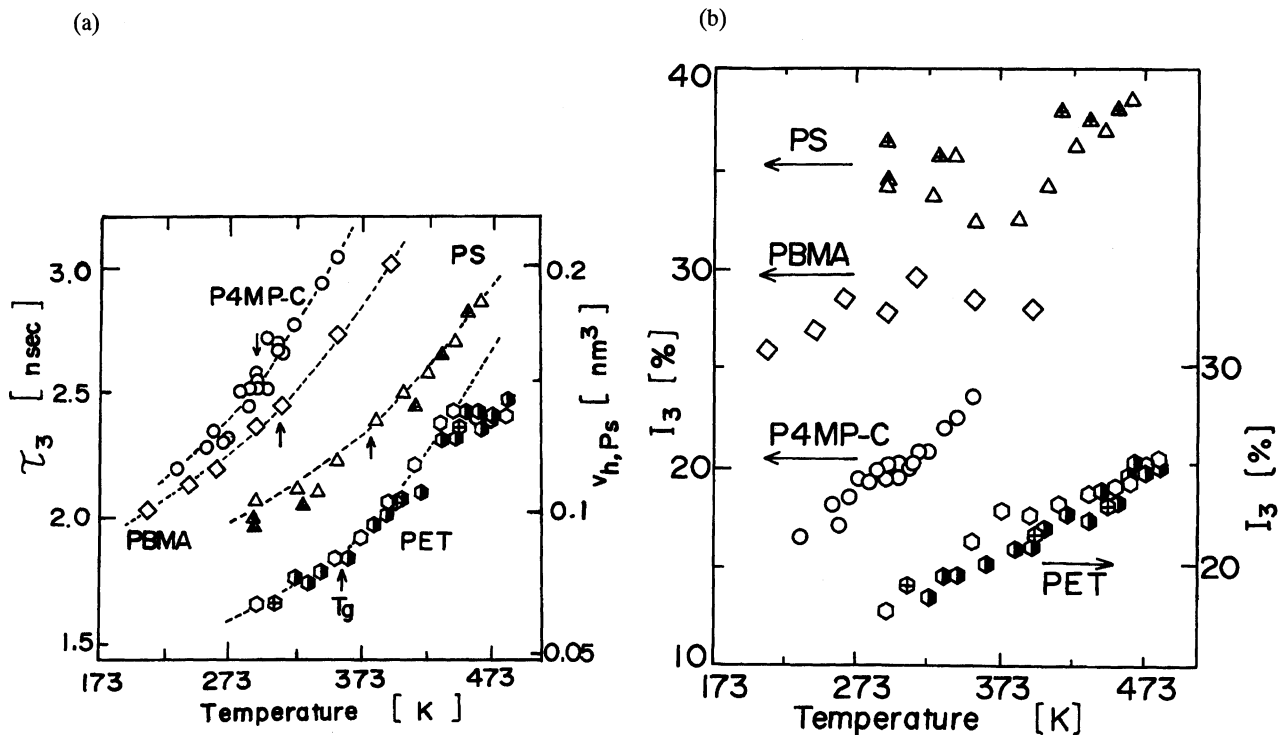


Fig. 2. Temperature dependence of τ_3 and I_3 for P4MP-C, PBMA, PS, and PET. \circ , \diamond , \triangle , and \square : 1st heating run; \triangle and \oplus : 1st cooling run; \bullet : 2nd heating run.

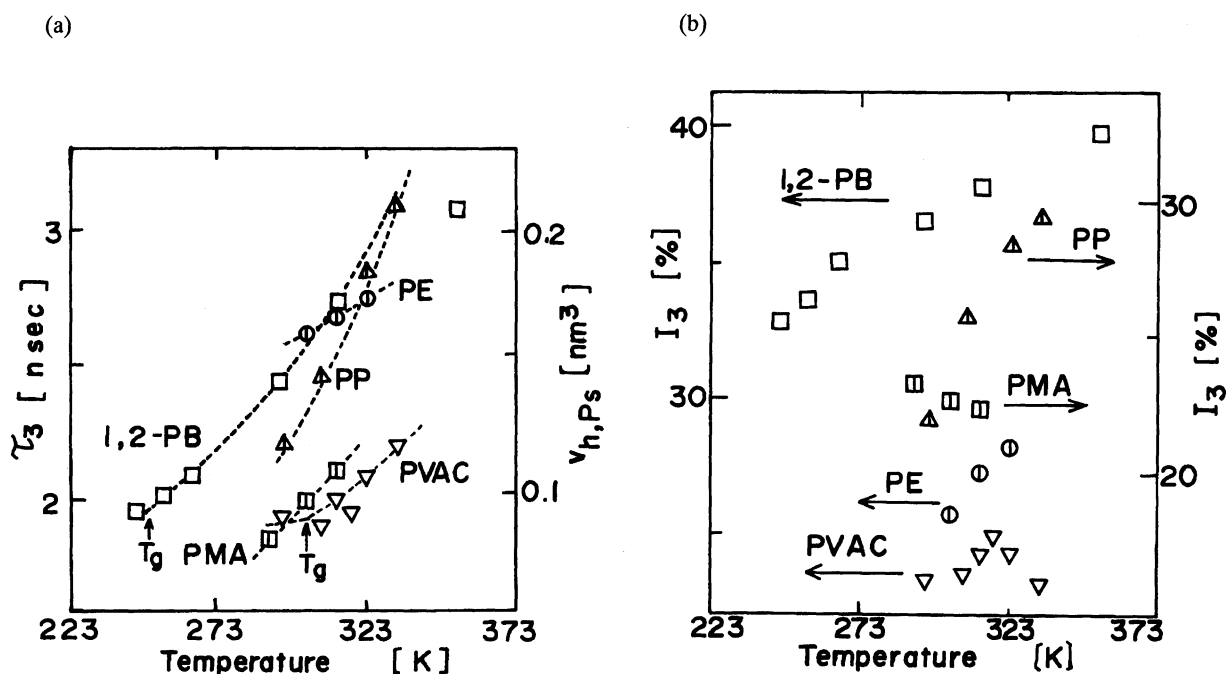


Fig. 3. Temperature dependence of τ_3 and I_3 for PE, PP, 1,2-PB, PMA, and PVAC.

and amine-cured epoxy polymers,¹⁶⁾ and has been interpreted as the temperature where the mortional correlation times of the polymers become on the order of 10^{-9} s, the same time scale as the σ -Ps lifetime. Above this transition the polymer has sufficient mobility to allow

the σ -Ps to "dig" itself a cavity, namely a Ps bubble, whereas below it the mortions are so slow that this possibility becomes prohibited.¹⁵⁾

Figures 2 and 3 show the temperature dependence of τ_3 and I_3 for the other polymers. τ_3 displayed fairly

clear changes at T_g , whereas I_3 displayed rather small or negligible changes at T_g . A higher-temperature transition was observed at 443 K and near 350 K for PET and 1,2-PB, respectively, where τ_3 started to level off and I_3 still increased.

The average volume of the microvacancies probed by α -Ps, $v_{h,Ps}$ [$= (4/3)\pi R^3$], was calculated from the following equation between τ_3 and the average radius R of microvacancies.^{2,3)}

$$\tau_3 = (1/2) [1 - (R/R_0) + (1/2\pi) \sin(2\Delta R/R_0)]^{-1} \quad (\text{ns})$$

$$R_0 = R + \Delta R, \quad \Delta R = 0.166 \text{ nm} \quad (3)$$

The thermal expansion coefficients of $v_{h,Ps}$, $\alpha(v_{h,Ps})$, defined as

$$\alpha(v_{h,Ps}) = (\partial \ln v_{h,Ps} / \partial T)_p \quad (4)$$

were calculated in appropriate temperature ranges above and below T_g , and are listed in Table 2. The values of $\alpha(v_{h,Ps})$ in the glassy and the rubbery states are one order of magnitude larger than the values of α_g and α_l , respectively. The dotted lines in Figs. 1, 2, and 3 were calculated from the $\alpha(v_{h,Ps})$ values by the integral form of Eq. 4 using the $v_{h,Ps}$ values at T_g as the initial values. The good agreement of the dotted lines with the experimental data indicates that the values of $\alpha(v_{h,Ps})$ for the glassy and the rubbery states are essentially constant in wide temperature ranges.

Figure 4 shows plots of $v_{h,Ps}$ versus CED for the polymers at 298 K together with the data for typical molecular liquids.¹⁷⁾ In this figure, the values of $v_{h,Ps}$ for the polymers at T_g are also plotted against values of CED at 298 K, neglecting the temperature dependence of CED. The Ps bubbles are believed to be formed in these liquids, and their size should be correlated with intermolecular force such as surface tension and CED.^{2,17)} This figure clearly shows that the data points for PDMS, 1,2-PB, and PET at the higher-temperature transition are on the correlation line (or zone) for Ps bubbles in the liquids, and that the data points for the polymers below, at, and not much above T_g are

Table 2. Thermal Expansion Coefficient of $v_{h,Ps}$ for Polymers in Rubbery and Glassy States

Polymer	$\alpha(v_{h,Ps})/10^{-3} \text{ K}^{-1}$	
	Glassy	Rubbery
PDMS	4.3	17
1,2-PB	—	5.3
PE	—	4.2
PP	—	15
PMA	—	11
P4MP-C	4.3	5.3
PBMA	3.2	4.3
PVAC	5.4	8.5
PET	3.7	6.1
PS	2.9	4.1

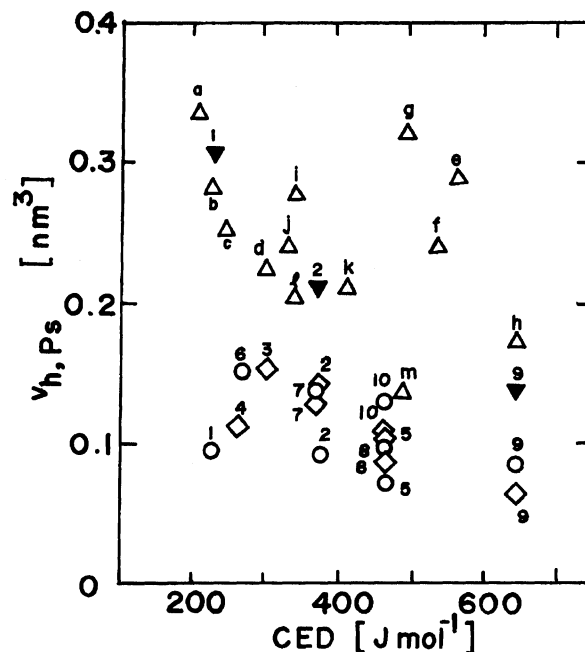


Fig. 4. Plots of $v_{h,Ps}$ versus CED for polymers and molecular liquids. For Polymers; O: at T_g ; ◇: at 298 K; ▼: at the higher-temperature transition of τ_3 . The figures are as in Table 1. For liquids; Δ: at 298 K. a: pentane, b: heptane, c: decane, d: cyclohexane, e: 2-propanol, f: 1-butanol, g: 2-methyl-2-propanol, h: cyclohexanol, i: acetone, j: methyl-ethylketone, k: benzene, l: ethylbenzene, and m: aniline.

much below the correlation line.

From the results and discussion mentioned above, it is reasonable to consider that the PA data measured at temperatures not much above T_g reflect the properties of pre-existing and momentarily frozen free volume holes rather than those of Ps bubbles.

Fraction of Free Volume Holes in Rubbery Polymers Probed by α -Ps. Fractional free volume f is generally expressed by

$$f = f_g + (\alpha_l - \alpha_g)(T - T_g), \quad (5)$$

where f_g is the fractional free volume at T_g . Williams-Landel-Ferry (WLF) fractional free volume, f_{WLF} , derived from viscosity theories, is often used, where f_g is taken as 0.025.^{18,19)}

For rubbery polymers, the volume fraction of free volume holes probed by α -Ps, $V_{F,Ps}$, is given by the product of $v_{h,Ps}$ and the concentration of free volume holes probed by α -Ps, $C_{h,Ps}$.

$$V_{F,Ps} = v_{h,Ps} C_{h,Ps} \quad (6)$$

I_3 contains information about $C_{h,Ps}$. Goldanskii et al. analysed the experimental data of PA from the view point of the kinetic model of positron trapping.^{20,21)} However, the Ps formation and the decay process were not clarified, and their treatment was based on many

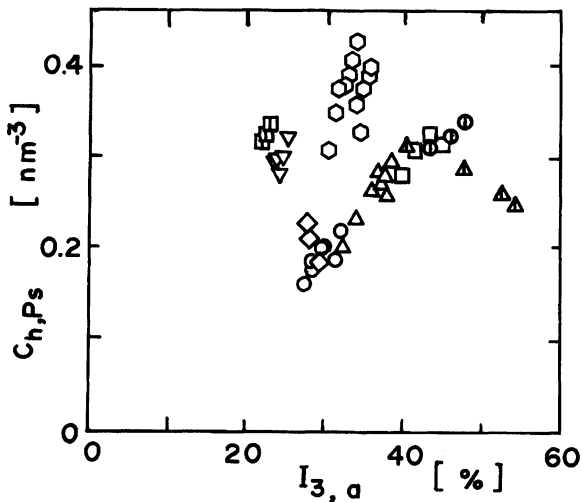


Fig. 5. Plots of $C_{h,Ps}$ evaluated on the assumption of $V_{F,Ps}=f_{WLF}$ versus $I_{3,a}$ in the rubbery state. \square : 1, 2-PB; \circ : PE; Δ : PP; \diamond : PMA; \circ : P4MP-C; \diamond : PBMA; ∇ : PVAC; \circ : PET; Δ : PS.

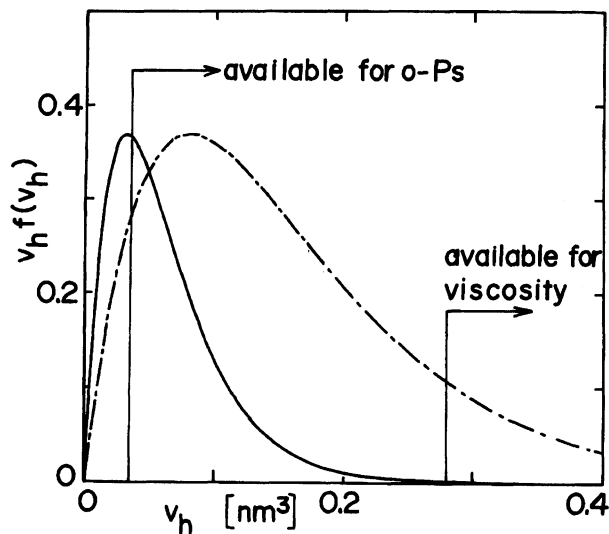


Fig. 6. Typical examples of the distribution function of fractional free volume.

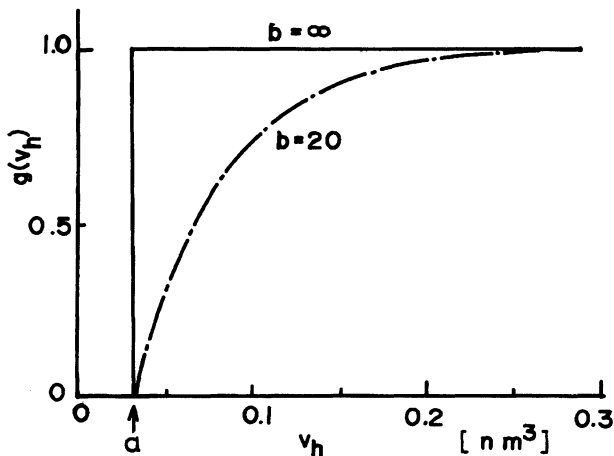


Fig. 7. Typical examples of $g(v_h)$.

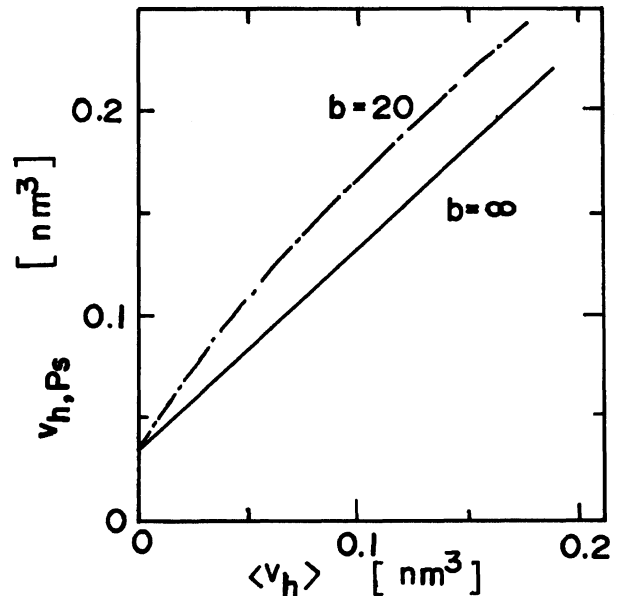


Fig. 8. Relation between $v_{h,Ps}$ and $\langle v_h \rangle$ for two assumed values of b in $g(v_h)$.

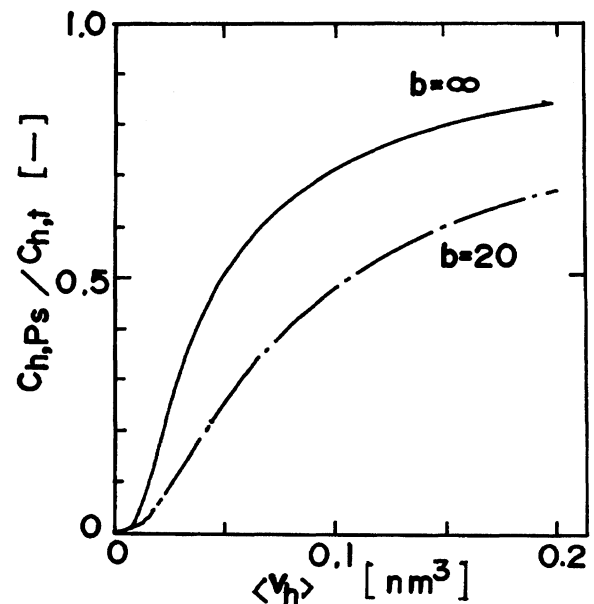


Fig. 9. Relation between $C_{h,Ps}/C_{h,t}$ and $\langle v_h \rangle$ for two assumed values of b in $g(v_h)$.

assumptions.

Assuming that $V_{F,Ps}$ could be taken equal to f_{WLF} , Jean et al. equated as follows, $C_{h,Ps} = [0.025 + (\alpha_1 - \alpha_g)(T - T_g)]/v_{h,Ps}$.^{5,6} They reported that a linear correlation exists between $C_{h,Ps}$ thus evaluated and I_3 with a proportionality constant $A(=C_{h,Ps}/I_3)$ of 0.018 nm^{-3} for amine-cured epoxy polymers.⁵ The same treatment was first reexamined for different kinds of rubbery polymers in this study. The $C_{h,Ps}$ thus evaluated is plotted against I_3 in Fig. 5. The long-lived component is assigned to o -Ps annihilating in the amorphous region. It has been found for semicrystalline polymers that I_3

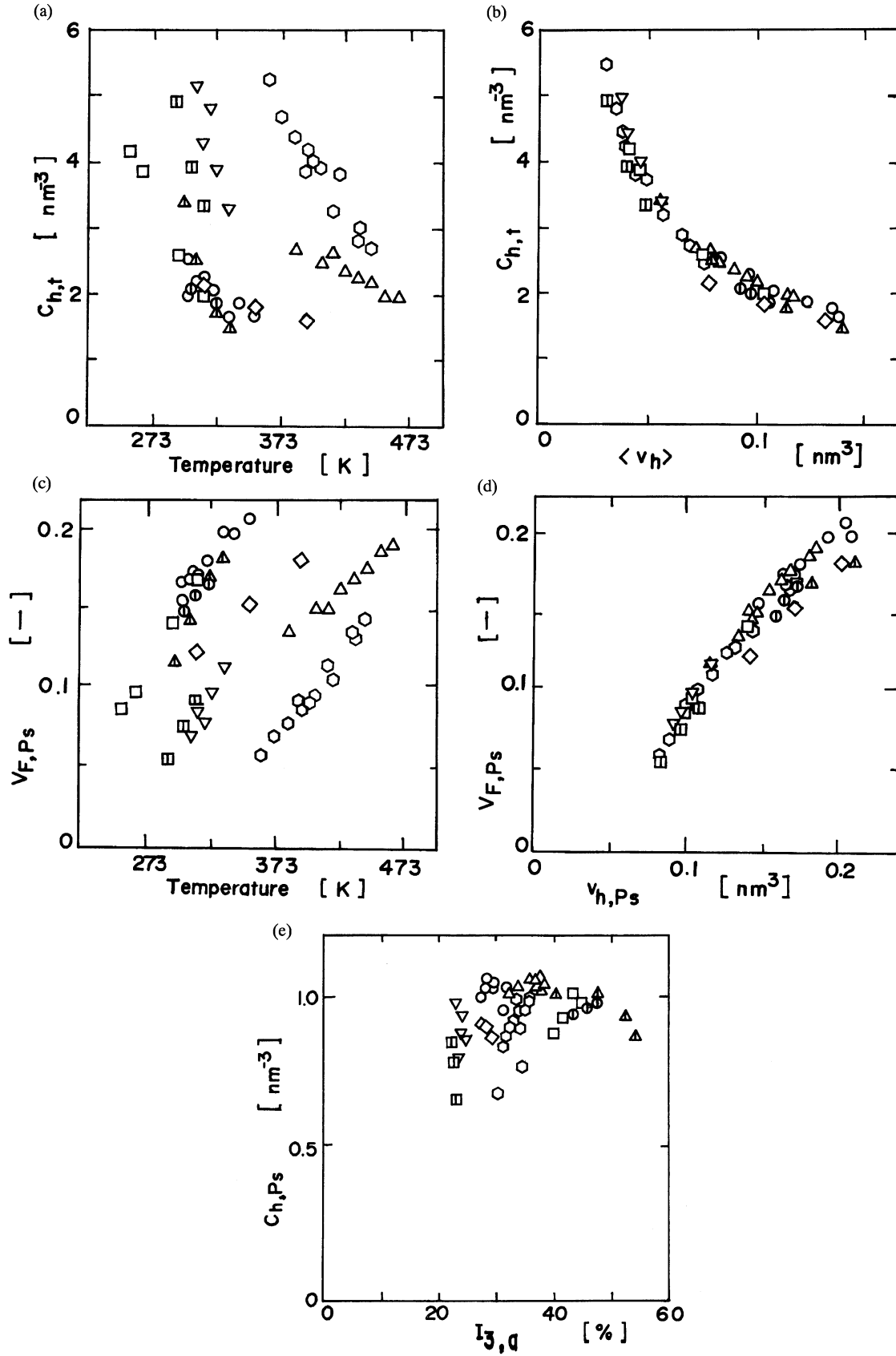


Fig. 10. Plots of (a) $C_{h,t}$ versus temperature, (b) $C_{h,t}$ versus $\langle v_h \rangle$, (c) $V_{F,Ps}$ versus temperature, (d) $V_{F,Ps}$ versus $v_{h,Ps}$, and (e) $C_{h,Ps}$ versus $I_{3,a}$ in the rubbery state below the higher-temperature transitions of τ_3 for $b=20$ in $g(v_h)$.
 □: 1,2-PB; ○: PE; △: PP; ◻: PMA; ○: P4MP-C; ◇: PBMA; ▽: PVAC; ⊙: PET; △: PS.

linearly depends on ϕ_a but τ_3 does not.²²⁾ In Fig. 5, I_3 values for the semicrystalline polymers are, therefore, corrected to give those in 100% amorphous samples, $I_{3,a}$, as

$$I_{3,a} = I_3 / \phi_a \quad (7)$$

As can be seen from Fig. 5, the value of A is not unique for these polymers; it varies from 0.005 nm^{-3} for PE to 0.014 nm^{-3} for PMA and is different from the value ($A=0.018 \text{ nm}^{-3}$) reported for the amine-cured epoxy polymers.⁵⁾ Therefore, the correlation between I_3 and $C_{h,Ps}$ evaluated by the above-mentioned method should be limited to a series of like polymers. The problem may lie in the assumption of $V_{F,Ps} = f_{WLF}$. It would be important to take the size distribution of the free volume holes into account. Viscosity requires free-volume holes equal to or larger than the size of a polymer chain segment, whereas α -Ps trapping requires those with the effective diameter larger than ca. 0.4 nm. Consequently, f_{WLF} involves a portion of free-volume distribution much larger in size than $V_{F,Ps}$ (see Fig. 6).

Now, we present another method to evaluate $C_{h,Ps}$ and $V_{F,Ps}$. The distribution function of the size of free volume holes, $f(v_h)$, for rubbery polymers is described by

$$f(v_h) = (1 / \langle v_h \rangle) \exp(-v_h / \langle v_h \rangle) \quad (8)$$

where $\langle v_h \rangle$ is a given mean size of free volume holes.²³⁾ Figure 6 shows typical examples of the distribution function of fractional free volume, $v_h f(v_h)$. The volume fraction of total free volume holes, which corresponds to the total area under the distribution curve in Fig. 6, is reasonably assumed to be equal to V_F calculated from Eq. 2.

$$C_h(v_h) = f(v_h) C_{h,t} \quad (9)$$

$$V_F = \int_0^\infty C_h(v_h) v_h dv_h = \langle v_h \rangle C_{h,t} \quad (10)$$

where $C_h(v_h)$ is the concentration of free volume holes with the size of v_h to $v_h + dv_h$ and $C_{h,t}$ is the concentration of total free volume holes. The critical volume which can accommodate α -Ps, a , has been shown by Bartenev et al.²⁴⁾ to be 0.033 nm^3 ($R=0.194 \text{ nm}$). It is not clear whether α -Ps is trapped in all the free volume holes larger than the critical volume, $a=0.033 \text{ nm}^3$, with equal probability. It is probable that α -Ps is trapped in a larger free volume hole with a larger probability. Therefore, taking the function $g(v_h)$ which describes the ease of trapping of α -Ps into consideration, volume fraction, average size, and concentration of free volume holes probed by α -Ps, $V_{F,Ps}$, $v_{h,Ps}$, and $C_{h,Ps}$, respectively, are described by Eqs. 11, 12, and 13.

$$V_{F,Ps} = C_{h,t} \int_a^\infty f(v_h) g(v_h) v_h dv_h = v_{h,Ps} C_{h,Ps} \quad (11)$$

$$v_{h,Ps} = \int_a^\infty v_h f(v_h) g(v_h) dv_h / \int_a^\infty f(v_h) g(v_h) dv_h \quad (12)$$

$$C_{h,Ps} = C_{h,t} \int_a^\infty f(v_h) g(v_h) dv_h \quad (13)$$

In this study, as $g(v_h)$, we tentatively use the following function,

$$g(v_h) = 1 - \exp[-b(v_h - a)] \quad (14)$$

Figure 7 illustrates $g(v_h)$ for two assumed values of b , ∞ , and 20. For these cases, $v_{h,Ps}$ and $C_{h,Ps}/C_{h,t}$ were calculated as a function of $\langle v_h \rangle$ from Eqs. 8, 12, and 13, and are shown in Figs. 8 and 9, respectively. For the polymers in the rubbery state, $C_{h,t}$, $C_{h,Ps}$, $V_{F,Ps}$ were calculated from Eqs. 8, 9, 10, 11, 12, 13, and 14, using the values of τ_3 and V_F at T . The results for the two assumed values of b are not much different each other. The results for $b=20$ are shown in Figs. 10a, 10b, 10c, 10d, and 10e. The following three points are noteworthy. First, with increasing temperature, $\langle v_h \rangle$ increases and $C_{h,t}$ decreases. This reveals that an increase in V_F with increasing temperature is ascribed to an increase in $\langle v_h \rangle$ and $C_{h,t}$ rather decreases. There is a clear tendency that the polymer with larger $\langle v_h \rangle$ has smaller $C_{h,t}$; the data points for all the polymers investigated are on a single correlation line, as shown in Fig. 10b. Second, there is a clear tendency that the polymer with larger $v_{h,Ps}$ has larger $V_{F,Ps}$; the data points for all the polymers are on a single correlation line, as shown in Fig. 10d, although the data for PE, PP, and PBMA display small deviations from the correlation line. This explains the clear correlation between diffusion coefficients of gases in the rubbery polymers and $v_{h,Ps}$.²⁵⁾ Third, there is no clear relationship between $C_{h,Ps}$ and I_3 , as shown in Fig. 10e. This fact implies that I_3 should not be taken a direct measure of the concentration of free volume holes. This may be supported by the fact that the shape of temperature dependence of I_3 is different from polymer to polymer, whereas that of τ_3 is similar among the polymers, as can be seen in Figs. 1, 2, and 3.

References

- 1) Y. C. Jean, "Positron and Positronium Chemistry," ed by Y. C. Jean, World Scientific, New Jersey (1990), p. 1.
- 2) S. T. Tao, *J. Chem. Phys.*, **56**, 5499 (1972).
- 3) M. Eldrup, D. Lightbody, and J. N. Sherwood, *Chem. Phys.*, **63**, 51 (1981).
- 4) Y. Kobayashi, K. Haraya, Y. Kamiya, and S. Hattori, *Bull. Chem. Soc. Jpn.*, **65**, 160 (1992).
- 5) Y. Y. Wang, H. Nakanishi, and Y. C. Jean, *J. Polym. Sci., Polym. Phys. Ed.*, **28**, 1431 (1990).
- 6) Q. Deng, C. S. Sundar, and Y. C. Jean, *J. Phys. Chem.*, **96**, 492 (1992).
- 7) T. Suzuki, Y. Ito, K. Endo, S. Fujita, Y. Masuda, and T. Egusa, *Int. J. Appl. Radiat. Isot.*, **39**, 53 (1988).
- 8) P. Kirkegaard, N. J. Pedersen, and M. Eldrup, "PAT-FITT-88, Riso-M-2740."

- 9) "Kagakubinran Oyohen," 2nd ed, ed by the Chemical Society of Japan, Maruzen, Tokyo (1973) pp. 832—839.
 - 10) M. S. Suwandi, T. Hirose, and A. Stern, *J. Polym. Sci., Polym. Phys. Ed.*, **28**, 407 (1990).
 - 11) "JSR RB Technical Report," Japan Synthetic Rubber, (1978), p. 9.
 - 12) D. W. van Krevelen, "Properties of Polymers," Elsevier, Amsterdam (1976), p. 129.
 - 13) Ref. 12, p. 65.
 - 14) A. Bondi, "Physical Properties of Molecular Crystals, Liquids, and Glasses," Wiley, New York (1968), p. 450.
 - 15) B. D. Malhotra and R. A. Pethrick, *Phys. Rev. B*, **28**, 1256 (1983).
 - 16) Y. C. Jean, J. C. Sandreczki, and D. P. Ames, *J. Polym. Sci., Polym. Phys. Ed.*, **24**, 1247 (1986).
 - 17) P. R. Gray, C. F. Cook, and G. P. Sturm, *J. Chem. Phys.*, **48**, 1145 (1968).
 - 18) M. I. Williams, R. F. Landel, and J. D. Ferry, *J. Am. Chem. Soc.*, **77**, 3701 (1955).
 - 19) R. N. Haward, *J. Macromol. Sci., Rev. Macromol. Chem. (C)*, **4**, 191 (1970).
 - 20) A. V. Goldanski, V. A. Onishuk, and V. P. Shantarovich, *Phys. Status Solidi A*, **102**, 559 (1987).
 - 21) A. V. Goldanski, V. A. Onishuk, V. P. Shantarovich, V. P. Volkov, and Yu. P. Yampolski, *Sov. J. Chem. Phys.*, **7**, 1011 (1991).
 - 22) H. Nakanishi and Y. C. Jean, *J. Polym. Sci., Polym. Phys. Ed.*, **27**, 1419 (1989).
 - 23) S. Trohalaki, L. C. Debolt, J. E. Mark, and H. L. Frish, *Macromolecules*, **23**, 813 (1990).
 - 24) G. M. Bartenev, A. Z. Varisov, V. I. Gol'danskii, A. D. Mokrushin, and A. D. Tsyganov, *Fiz. Tverd. Tela (Leningrad)*, **12**, 3454 (1970).
 - 25) K. Tanaka, M. Katsube, H. Kita, K. Okamoto, O. Sueoka, and Y. Ito, *Polym. Prep. Jpn.*, **41**, 1560 (1992).
-